Supporting Information

Dipoppa and Gutkin 10.1073/pnas.1303270110

SI Text

Neural Models

The network is made of point neurons the dynamics of which are described by the Quadratic Integrate and Fire (QIF) equation, the normal form of any type 1 neuron (1)

$$\tau\frac{dv}{dt}=v^2-I_i+I_e(t), \qquad [S1]$$

and is combined with a reset equation

$$v(t)=V_t\rightarrow V_r, \qquad [S2]$$

where τ is the membrane time constant, I_i a constant negative current representing local inhibition, $I_e(t)$ the excitatory synaptic current, V_t the spike threshold, and V_r the reset membrane potential. Here, v is scaled to be a nondimensional variable. Because $I_i>0$, the neuron is in an excitable regime, i.e., in the absence of external excitatory input the only stable point is the resting potential $-\sqrt{I_i}$. When v attains the threshold V_t, a spike is emitted and a postsynaptic current (PSC) is transmitted to the output neurons. We set the following parameters: $V_r=-20$, $V_t=20$, and $I_i=1$.

The excitatory input is decomposed into three components:

$$I_e(t)=I_r(t)+I_s(t)+I_{ba}(t), \qquad [S3]$$

where $I_r(t)$ is the recurrent input due to other neurons in the network, $I_s(t)$ is the input from external stimuli, and $I_{ba}(t)$ is a nonspecific background input. Each of the three currents corresponds to a sum of delta-pulse PSCs coming from the presynaptic neurons:

$$I(t)=\sum_a\sum_{\{t_n\}}J_a\tau\delta(t-t_n), \qquad [S4]$$

where J_a is the synaptic strength and $a\in\{r,s,ba\}$ denote recurrent, sensory stimulus, and background activity synaptic input. Such fast PSCs represent AMPA excitation. Synaptic activity in the figure is represented in terms of synaptic units (s.u.) with 1 s.u. $=J_r$.

External Oscillation

All of the neurons receive a spike train generated by independent Poisson processes with the rate function $\nu_s(t)$. $\nu_s(t)$ and oscillates with period T_s (frequency ν_s):

$$\nu_s(t)=\begin{cases}\left(\frac{1-\gamma}{\gamma}\beta+1\right)\nu_0, & 0<t<\gamma T_s\\ (-\beta+1)\nu_0, & \gamma T_s<t<T_s\end{cases}, \qquad [S5]$$

where $0\le\beta\le1$ scales the wave amplitude, and $0\le\gamma\le1$ is the duty cycle measuring the duration of the "excitatory" phase. Oscillation input is represented in Fig. 4*D* and Fig. S4*B* in terms of $\beta\nu_0\,J_{ba}/J_r$ in s.u. The mean rate over a period T_s is ν_0, giving the average background frequency. Note that this oscillation has a nonsinusoidal shape according to the notion of amplitude asymmetry as previously suggested experimentally (2, 3).

Network Models

The single-population unit network is made up of N identical sparsely coupled neurons. Each neuron in the network receives synaptic inputs with recurrent synaptic strength J_r from cN other excitatory neurons, where c is the probability of connection. Neurons receive excitatory inputs also from external background activity, with background synaptic strength J_{ba}. The background activity can be modulated by an asynchronous rate ν_0 or by an external oscillatory rate $\nu_s(t)$, as described previously. Finally, neurons can also receive input from external sensory stimuli with stimulus synaptic strength J_s, average firing rate ν_1, and duration ΔT_s. Parameters of the network are chosen such that the resting state is $f<5$ Hz and the persistent state is $f\sim20$ Hz. Transient sensory excitation can activate the network with a down–up transition from the resting state to the persistent state. The parameters of the network, when is not otherwise specified, are fixed as follows: $N=100$, $c=0.2$, $J_r=0.297$, $\nu_0=80$ Hz, $J_{ba}=0.2$, $\nu_1=7.8$ Hz, $J_s=1.5$, $\Delta T_s=100$ ms, and $\tau=20$ ms.

Two-Population Unit Networks

In the local network, the parameters for each population are equivalent to those of the single-population unit. The sequence of frequencies for the oscillation that modulates the background input of both population are: gamma with $\nu_s=45$ Hz, theta with $\nu_s=6.5$ Hz, and alpha with $\nu_s=10$ Hz. The oscillations have the following parameters: $\gamma=0.2$ and $\beta=0.625$.

The parameter of the bihemispheric network are: $N=100$, $c=0.2$, $J_r=0.26$, $\nu_0=93$ Hz, $J_{ba}=0.151$, $\nu_1=56$ Hz, $J_s=1.5$, $\Delta T_s=50$ ms, and $\tau=20$ ms. The most relevant difference with respect to the local network is that stimulus synaptic strength is larger. This choice is not related to the fact that the model is a bihemispheric network but with the fact that the memory is cleared with the match stimulus instead that with the alpha oscillations. It is possible to have the same parameters of the local network if the memory in the bihemispheric network is cleared by an alpha oscillation at the end of the task. The frequency for the oscillation that modulates the background input of population R is alpha with $\nu_s=10$ Hz, $\gamma=0.2$, and $\beta=0.625$. The sequence of oscillations that modulate the background of population B have parameters: $\nu_s=45$ Hz, $\gamma=0.5$, and $\beta=0.16$ for gamma ; $\nu_s=6.5$ Hz, $\gamma=0.5$, and $\beta=0.16$ for theta. Note that the different parameters in the bihemispheric network require lower coherence in the theta oscillation to allow memory maintenance. In the bihemispheric network where the frequency is modulated only in space (Fig. S6), population B receives only a frequency in the gamma range during all of the duration of the task with parameters $\nu_s=45$ Hz, $\gamma=0.2$, and $\beta=0.625$.

Measure of Erasing, Blocking, and Gating Probabilities

Erasing probability [$P(erase)$] and blocking probability [$P(block)$] represented in Fig. 3*A* are defined as follow. $P(erase)$ is the probability that the network has robust sustained activity before the oscillatory modulation is turned on (in the interval 450–550 ms) and that then is deactivated in the interval 950–1,050 ms. In this protocol, the neurons first receive external nonmodulated rate noise (because the noise comes from independent sources, this background is asynchronous). A sensory external stimulus, presented during 50–150 ms, is able to activate the network. From 550 ms on, the external noise is modulated by an oscillation of frequency ν_s, the fluctuations induce oscillatory correlations and hence partial synchrony in the input.

$P(block)$ is the probability that the network is not activated by the transient stimulus and so there is no sustained activity. In this protocol the external noise is modulated throughout the simulation by an external oscillation of frequency ν_s. The sensory

stimulus is presented during 50–150 ms, hence when the external noise is oscillating.

The probability of the gate-in ($P_{g.i.}$), selective-gating ($P_{s.g.}$), and gate-out ($P_{g.o.}$) modes represented in Fig. 3*A* are defined as follow: $P_{g.i.} = [1 - P(erase)][1 - P(block)]$, $P_{s.g.} = [1 - P(erase)]P(block)$, and $P_{g.o.} = P(erase)P(block)$. The values of the gating modes in Fig. S2 *F* and *E* are the maximal values of the curves in Fig. S2 *A* and *B*. The errors in Fig. S2 *E* and *F* are defined as the shift in frequency needed for a decrease in the selective mode probability of at least 5% with respect to the peak in Fig. S2 *A* and *B*.

Measure of Operation and Task Performance

In the local network in Fig. S3*A* (bihemispheric network in Fig. S5*A*) we assess the performance of the operations in the following way: load is executed with success if population *B* is in the persistent state after 700 ms from sample offset during 850–950 ms (800–900 ms). Maintain is executed with success if population *B* is in the persistent state after 700 ms from sample offset during 1,750–1,850 ms (1,650–1,750 ms). Block distractor is executed with success if population *R* is in the resting state during 1,750–1,850 ms (1,650–1,750 ms). Clear is executed with success if population *B* is in the resting state after 700 ms from sample offset during 2,650–2,750 ms (2,500–2,600 ms). We assess the overall task performance for the local network in Fig. 4*D* (for the bihemispheric network in Fig. S4*B*) in the following way: if previous to the match presentation during 1,750–1,850 ms (1,650–1,750 ms) the population *B* is in a persistent state and the population *R* is in the resting state it is considered a successful trial. If both populations *B* and *R* are in the persistent state and the network performs successfully at chance level, the trial is considered half failure. If population *B* is in the resting state, whatever is the state of population *R,* the trial is considered a failure.

Parameter Scaling

The measures of erasing and blocking probability have been performed with an appropriate scaling of the parameters in the single-unit population network. In the analysis where γ is varied (Fig. S2 *A* and *E*), to maintain a fixed amount of excitation in the excitatory phase of the oscillation, we set the value of β such that

$$\frac{1}{T_s}\int_0^{\gamma T_s} [\nu(t) - \langle \nu(t) \rangle] dt = (1-\gamma)\beta\nu_0 = K_0\nu_0, \qquad \textbf{[S6]}$$

where K_0 is a constant term. Because ν_0 is constant, this leads to the scaling relation: $\beta = K_0/(1-\gamma)$, with $K_0 = 0.5$. In the analysis where τ is varied (Fig. S2 *B* and *F*), to compare network with similar activation probability, we scaled all of the temporal parameter of the network and the stimuli (not of the task timing, but this does not change remarkably the results): $\nu_1 = K_1/\tau$ with $K_1 = 0.156$, $\Delta T_s = K_2\tau$ with $K_2 = 5$, and $\nu_0 = K_3\tau$ with $K_3 = 1.6$. In the analysis where *N* is varied (Fig. S2*C*), to maintain a fixed number of presynaptic inputs per neuron, we fixed $N = K_4/c$ with $K_4 = 20$. In the analysis where J_r is varied (Fig. S2*D*) no other parameter is varied.

Numerical Analysis

All of the numerical results are obtained by algorithm run in Python on a cluster of computers. The differential equations are integrated with Euler steps of $dt = 0.1$ ms. The mean population firing rate ν and the represented synaptic input are computed over population average in 10 ms. Persistent and resting states are discriminated by half of the minimal frequency of the persistent state predicted by mean field theory at the bifurcation point. This corresponds to $\nu^*_{ps}/2$ (see details in *Mean-Field Analysis of the Bistable Network*) and depends on the network parameters.

The time-frequency spectrograms of the synaptic inputs are computed through the function "specragm" in the library Pyplot of Matplotlib, available online. This function computes a spectrogram for sliding windows of length 1 s, shifted by 80 ms, and tapered by a Hanning window. The frequency resolution is 0.25 Hz. For the local network analysis, we first summed the average synaptic input of populations *B* and *R* and then we computed the spectrogram. For each time bin we normalized the density of the power spectrum for the frequency range 5–35 Hz (Fig. 4*C*). For the bihemispheric network analysis, we first computed separately the average synaptic input of each of the populations *B* and *R* (Fig. S4) and then we computed the two corresponding spectrograms. For each time bin and for each spectrogram we normalized the density of the power spectrum for the frequency range 5–35 Hz. We finally subtracted the resulting spectrogram of population *B* from the spectrogram of population *R* (Fig. 5*B*).

Statistics for each estimated parameters were computed over 30 connectivity realizations (each neuron receives same number of input connections) with 100 trials for each realization of connectivity. Errors (SEM) are computed over the averages of the values for the different connectivity realizations.

Controlling for Effects of Average Excitation during Oscillatory Inputs

We provide here a detailed description of a control test (Fig. S1) where, to make sure that the induced erasing for alpha range is not due to transient decreases of the excitatory input at the low phases of the oscillation, we modified the protocols of Fig. 2 such that the oscillation is replaced by a constant rate equivalent to the minimal value of the oscillatory input.

We find that the persistent state is maintained (not erased) but is prevented from being activated by the sensory stimulus. Compared with the result with alpha oscillation ($\nu_s = 10$ Hz, Fig. 2*C*), the maintenance of the persistent activity proves that the erasing-by-oscillation effect does not originate from the decrease in excitation during the low phase of the oscillation. In fact, the low phase of the oscillation has the same firing rate of the decreased constant asynchronous input tested here. Note that a decrease in excitation is equivalent to an increase of inhibition, and this proves that the effect of oscillations described here is not explainable by the inhibition-induced gating. Although the decrease in the constant level of background input leads to a failure to activation similar to what happens under theta and alpha oscillations ($\nu_s = 6.5$ Hz, Fig. 2*B*, and $\nu_s = 10$ Hz, Fig. 2*C*), in these last cases (but not in the constant-rate case) the sensory stimulus causes a strong transient spiking response. This transient increase, observed also in experimental data (4), indicates that the failure of activation under oscillations is not based on a simple lack of excitation as should be in the inhibition-induced gating paradigm proposed by the majority of previous models.

Scaling of Effects of Oscillatory Input with Network Size and Synaptic Strength

We studied the values of *P*(*block*) and *P*(*erase*) as a function of the oscillation duty cycle γ (Fig. S2*A*). We find that the *P*(*erase*) scales down and the *P*(*block*) is largely invariant as the excitation profile during the oscillatory cycle gets flatter (γ increases). It is interesting to note that the upper bound of the band for the probability curves (mid value at ∼ 13 Hz) is constant for different values of γ. Instead, the lower bound (5 Hz $< \nu_s <$ 10 Hz) of the erasing band depends significantly on the value of γ. In particular, for *P*(*erase*) there is a whole frequency range where the erasing probability falls to zero for high values of γ. We surmise that for low-oscillation frequencies the persistent activity erasing is elicited by the rapid transient synchronization created by strong rapid excitatory input.

We studied the values of *P*(*block*) and *P*(*erase*) (Fig. S2*B*). We found that τ controls the frequency range and tuning of *P*(*block*) and *P*(*erase*). Note that increasing τ leads to a decrease of the persistent-state firing rate ν, as reported in the inset of Fig. S2*B*.

In the simulations presented in the main text we use networks with 100 neurons each. We performed test simulations with progressively larger networks and found that the effects of the oscillatory input on the blocking and erasing of the persistent activity remained qualitatively invariant with network size: the frequency tuning for erasing remained largely the same (Fig. S2*C*).

We varied the synaptic strengths we found that the upper bound for the probability curves is approximately invariant, yet the amplitudes of the probabilities for the two operations are modulated by J_r (Fig. S2*D*). Note that increasing J_r leads to an increase of the persistent-state firing rate ν, as reported in the inset of Fig. S2*D*.

Additional information for the Local Network

We statistically assessed the performance of the operations load, maintain, block distractor, and clear (*Materials and Methods*) for the local network (Fig. S3*A*). Note that all of the operations are performed with high probability. The phase (relative to the start of theta increase) optimal for block distractor (270°, Fig. S3*B*) was selected. In particular, we computed the block distractor performance as a function of the phase of the theta oscillation and the performance of the clear performance as a function of the phase of the alpha oscillation (Fig. S3*B*). The block distractor performance is maximal when the offset of the excitatory phase of the oscillatory cycle coincides with the offset of the distractor stimulus (Fig. S3*C*, *Top*). This is consistent with an excess of excitation and thus, of synchronization at the offset of the distracting stimulus, in line with previous theoretical works (5, 6).

Additional information for the Bihemispheric Network

We present in Fig. S4*A* the rastergram of the bihemispheric network showing that this sequence of gating modes enables the WM system to perform successfully all of the operations of the DMS task with distractors, and to be robust against strong distractors (as opposed to inhibition-induced gating; e.g., refs. 7, 8). We computed separately the spectrograms of the ipsilateral (irrelevant or *R*) population (Fig. S4*D*) and that of the contralateral (relevant or *B*) population (Fig. S4*C*). The spectrograms are obtained from each of the average synaptic input of the two populations (*Materials and Methods*).

We statistically assessed the performance of the operations load, maintain, block distractor, and clear (Fig. S5*A*). We can see that the alpha oscillations are quite effective in blocking the memory activation by the distractors. This is in line with data associating alpha with functional inhibition of nonrelevant stimuli. We computed the average amplitude (over 300 trials) of the transient response in the ipsilateral (*R*) population (maximal value of the firing rate following the distractor presentation) as a function of the phase of the alpha oscillation. We then computed the relative amplitude with respect to the mean to estimate the modulation (Fig. S5*B*). We report a modulation of up to 23% of transient stimulus response as a function of the alpha phase. This result seems consistent with the fact that the phase of a TMS-induced alpha oscillation in the human visual cortex modulates the probability of illusory perception (phosphene) of up to 15% (figure 2 c and d in ref. 9) associated with a change in cortical excitability (9).

Modulating the Frequency only in Space in the Bihemispheric Network Model Enables the WM Performance

We want to demonstrate that it is possible to execute a DMS with distractors in a bihemispheric network by modulating the frequency of the external oscillation only in space and not in time. The paradigm is similar to the one described for Fig. 5, where the population selective to the irrelevant information receives alpha-band oscillations (10 Hz) during all of the duration of the task. However, the population selective to the relevant information is subject to a gamma-band oscillation (45 Hz) during all of the duration of the task and not only during load and clear as in Fig. 5. The simulated LFPs and the gating modes are represented together (Fig. S6*A*). The rastergrams from both the relevant and the irrelevant networks show that the model correctly executes the various stages of the task (Fig. S6*B*): the sample stimulus to population B at time 50–100 ms, the distractor stimulus to population R at time 900–950 ms, and match stimulus to population B at time 1,750–1,800 ms.

Memory Performance of our Model as a Function of the Number of Items to be Retained

We describe here the performance of our network in maintaining N_i memorized items. Consider the multiitem network described in Fig. 4 extended to a larger number of independent populations (at least N_i populations). From Fig. 3*A* (red star) we have that, at 6.5 Hz, each item has a probability to be maintained [the complement of probability to be erased $= 1 - P(erase)$] during theta oscillation that is $P_m^1 = 0.93 \pm 0.03$. This means that the probability to maintain N_i items is $P_m^{N_i}$ (Fig. S7, continuous red line) that decreases with N_i. If we want such probability to be beyond chance for $N_i = 7$ and below chance for $N_i = 8$, we can impose $P_m^{7.5} = 0.5$. This yields the value $P_m^1 = 0.91$ that is within the error of our measurement (Fig. S7, dashed red line) and would correspond to a value of the oscillation frequency 6.5 Hz $< \nu_s < 7$ Hz that is within the range of the theta frequency. As we can see here, the average number of items that can be maintained by the WM system can be regulated by the frequency of the theta oscillation.

Mean-Field Analysis of the Bistable Network

We want to compute the value of the membrane potential threshold $\nu_D = \nu_{ps}^*/2$ that discriminates if the network is in the persistent activity or the resting state. This can be derived from mean-field analysis for an infinite size network of QIFs neurons (10). For simplicity we consider here $V_t = \infty$ and $V_r = -\infty$. In the infinite network, if the system is set in a stationary state, then each neuron receives a constant background input $I_{ba} = \langle I_{ba}(t) \rangle$ and a constant recurrent input $I_r = \langle I_r(t) \rangle$. If $I_{ba} < 1$ (subthreshold background activity) the system has at least a stable solution with $\nu_{rs} = 0$, corresponding to the resting state. In fact, if the second-order moments given by the input fluctuations are taken in account, the resting state mean rate is $\nu_{rs} > 0$ (this does not change qualitatively the results). From Eqs. **S1** and **S3** in the main text it is possible to calculate the mean-mean field equations. The solutions of the mean-field equations are

$$\nu_{+,-}^{ps} = \frac{I_r \pm \sqrt{I_r^2 - 4\tau^2\pi^2(1 - I_{ba})}}{2\pi^2\tau^2}.$$

The upper solution exists for $I_r > I_r^*$ with $I_r^* = 2\tau\pi\sqrt{1 - I_{ba}}$. The upper solution is stable and corresponds to the persistent state. Here I_r^* corresponds to the bifurcation point of the system whose firing rate is

$$\nu_{ps}^* = \sqrt{1 - I_{ba}} \big/ (\pi\tau).$$

1. Ermentrout B (1996) Type I membranes, phase resetting curves, and synchrony. *Neural Comput* 8(5):979–1001.
2. Nikulin VV, et al. (2007) A novel mechanism for evoked responses in the human brain. *Eur J Neurosci* 25(10):3146–3154.
3. Mazaheri A, Jensen O (2008) Asymmetric amplitude modulations of brain oscillations generate slow evoked responses. *J Neurosci* 28(31):7781–7787.
4. Miller EK, Erickson CA, Desimone R (1996) Neural mechanisms of visual working memory in prefrontal cortex of the macaque. *J Neurosci* 16(16): 5154–5167.
5. Gutkin BS, Laing CR, Colby CL, Chow CC, Ermentrout GB (2001) Turning on and off with excitation: The role of spike-timing asynchrony and synchrony in sustained neural activity. *J Comput Neurosci* 11(2):121–134.

6. Laing CR, Chow CC (2001) Stationary bumps in networks of spiking neurons. *Neural Comput* 13(7):1473–1494.
7. Compte A, Brunel N, Goldman-Rakic PS, Wang X-J (2000) Synaptic mechanisms and network dynamics underlying spatial working memory in a cortical network model. *Cereb Cortex* 10(9):910–923.
8. Brunel N, Wang X-J (2001) Effects of neuromodulation in a cortical network model of object working memory dominated by recurrent inhibition. *J Comput Neurosci* 11(1): 63–85.
9. Dugué L, Marque P, VanRullen R (2011) The phase of ongoing oscillations mediates the causal relation between brain excitation and visual perception. *J Neurosci* 31(33): 11889–11893.
10. Hansel D, Mato G (2001) Existence and stability of persistent states in large neuronal networks. *Phys Rev Lett* 86(18):4175–4178.

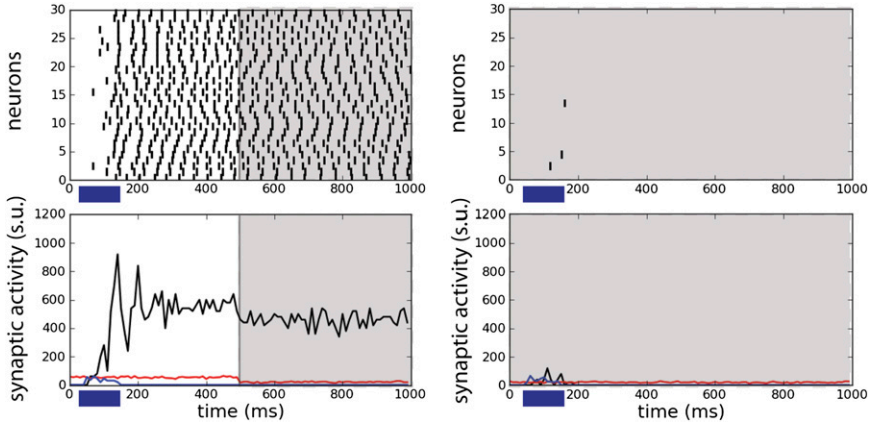

Fig. S1. Blocking and erasing are not a consequence of the firing rate modulation. *Upper* shows the rastergram of 30 representative neurons, and *Bottom* shows average population input from recurrent connections (black), background activity (red), and external stimulus (blue) in arbitrary/normalized units. The background activity is decreased either after the stimulus presentation (*Left*) or before (*Right*). Here the rate of the Poisson inputs is reduced to the lowest amplitude during the oscillation, and the persistent state is maintained. Transient stimulus (blue bars) is not able to evoke a strong response transient without persistent activation.

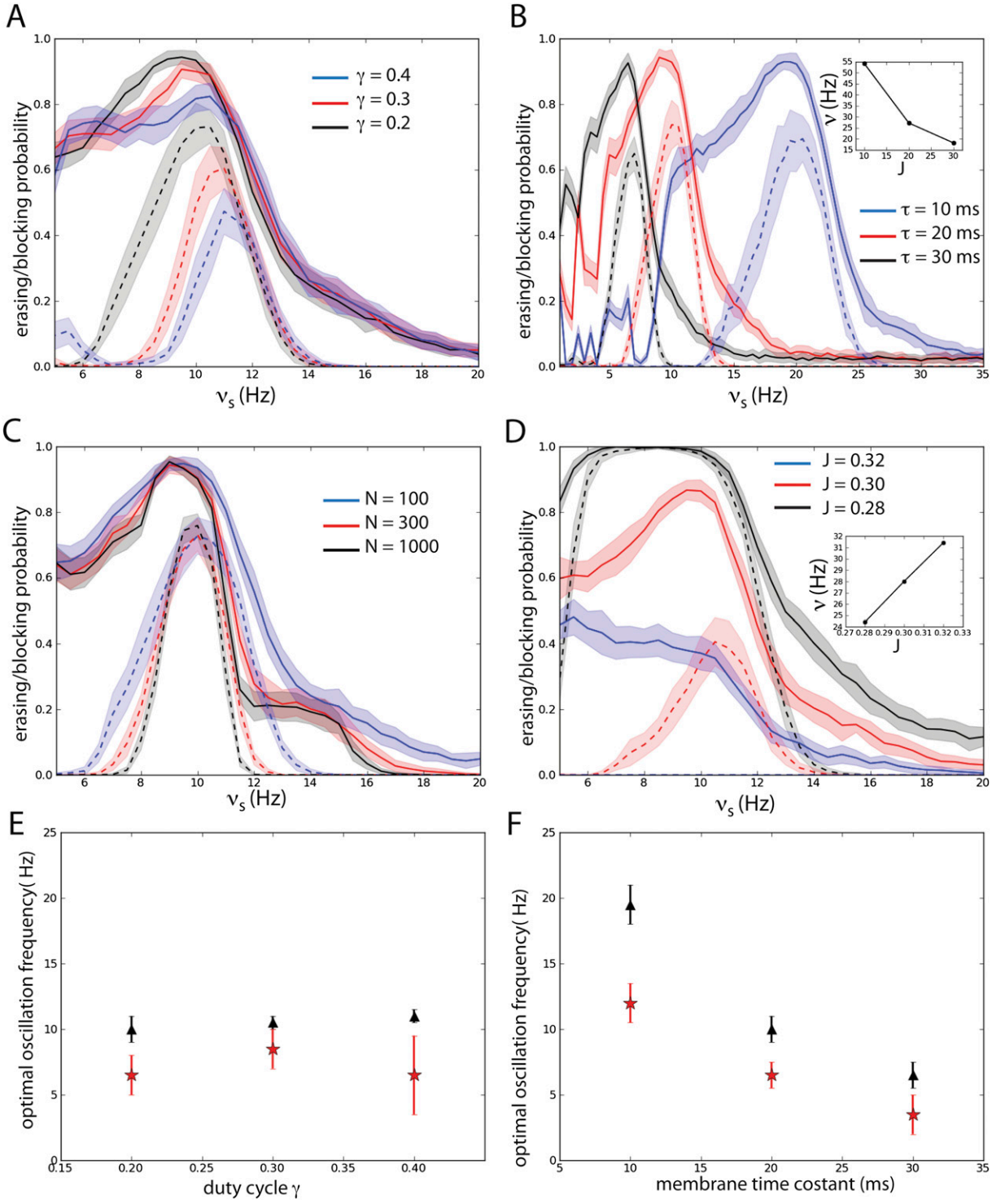

Fig. S2. Influence of various network parameters on erasing and blocking probabilities. *P*(*erase*) (dashed lines) and *P*(*erase*) (continuous lines) as a function of (*A*) the duty cycle γ, (*B*) the membrane time constant τ (*Inset*, average population firing rate ν for each value of τ), (*C*) the network size *N*, and (*D*) the recurrent synaptic strength J_r (*Inset*, average population firing rate ν for each value of J_r). (*E*) Optimal values of the selective-gating mode (red stars) and of the gate-out modes (black triangles) are approximately unvaried with respect to the duty cycle γ. (*F*) Optimal values of the selective-gating mode (red stars) and of the gate-out modes (black triangles) strongly correlate with the membrane time constant τ.

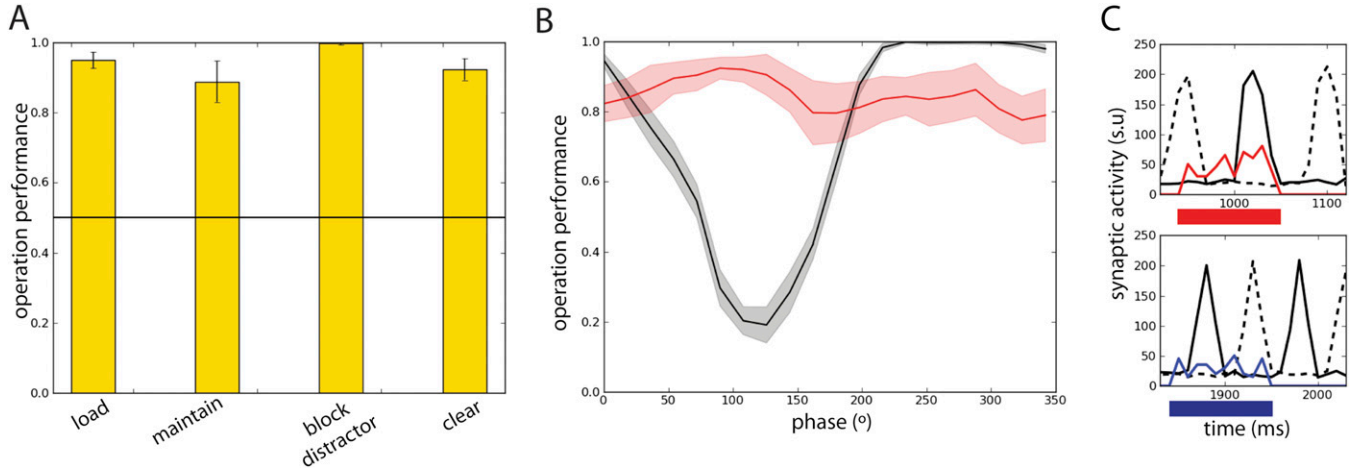

Fig. S3. (*A*) Summarized working memory performance of the four delayed match-to-sample task operations for the local network. (*B*) Performance of the block distractor operation (black line) as a function of the theta phase relative to the distractor stimulus and clear operation (red line) as a function of the alpha phase relative to the match stimulus. (*C*, *Upper*) Theta oscillation with best (continuous black line) and worst (dashed black line) phase-induced distractor block distractor performance (red line), (*Bottom*) alpha oscillation with best (continuous black line) and worst (dashed black line) clear performance (blue line marks the synaptic activity induced by the match stimulus).

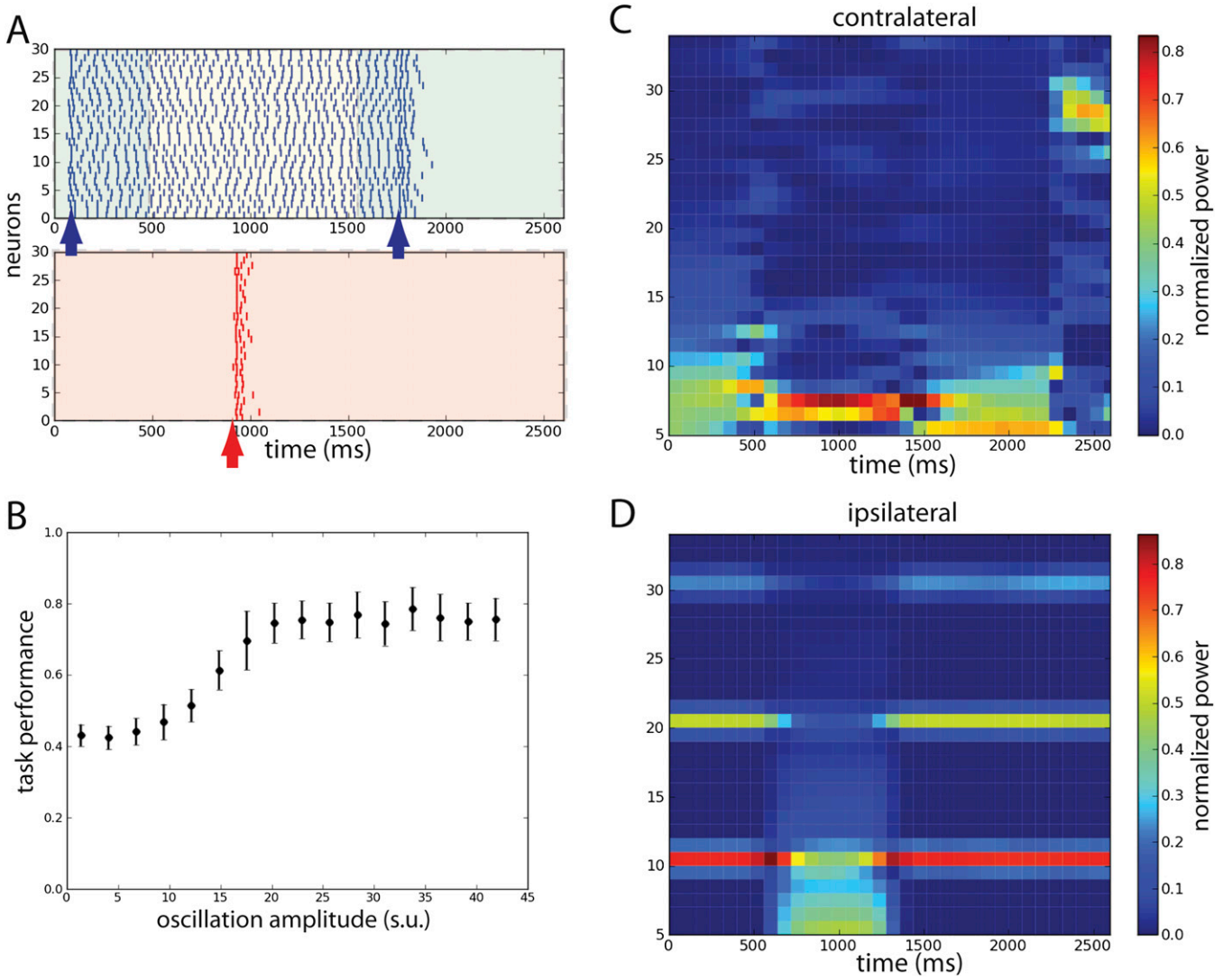

Fig. S4. Supplemental plots of the bihemispheric network in Fig. 5. (*A*) Rastergrams of 30 representative neurons for each population of the bihemispheric network. (*B*) Task performance of the bihemispheric network described by a psychometric curve with respect to the oscillation amplitude in the ipsilateral (irrelevant) population. Spectrogram of the (*C*) contralateral and (*D*) ipsilateral populations in the bihemispheric network.

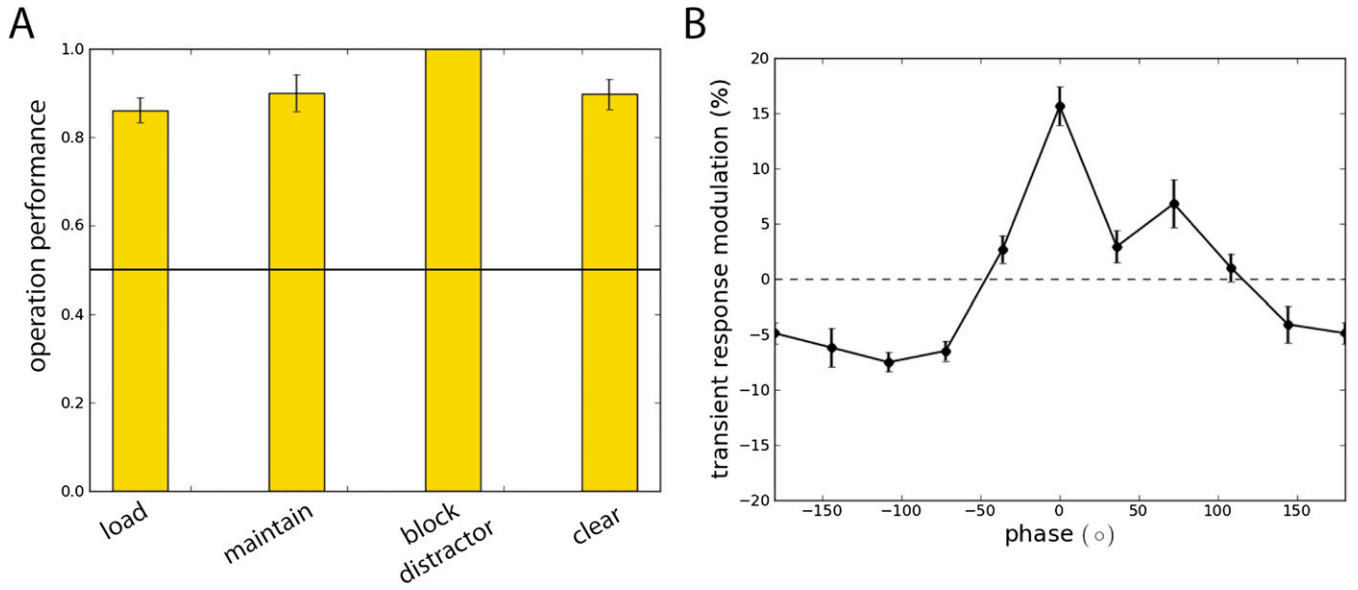

Fig. S5. (*A*) Summarized working memory performance of the four delayed match-to-sample task operations for the bihemispheric network. (*B*) Modulation (with respect to the mean) of the peak of the transient response to the distractor in the ipsilateral population as a function of the phase of the alpha oscillation. Compare with figure 2 c and d in ref. 9.

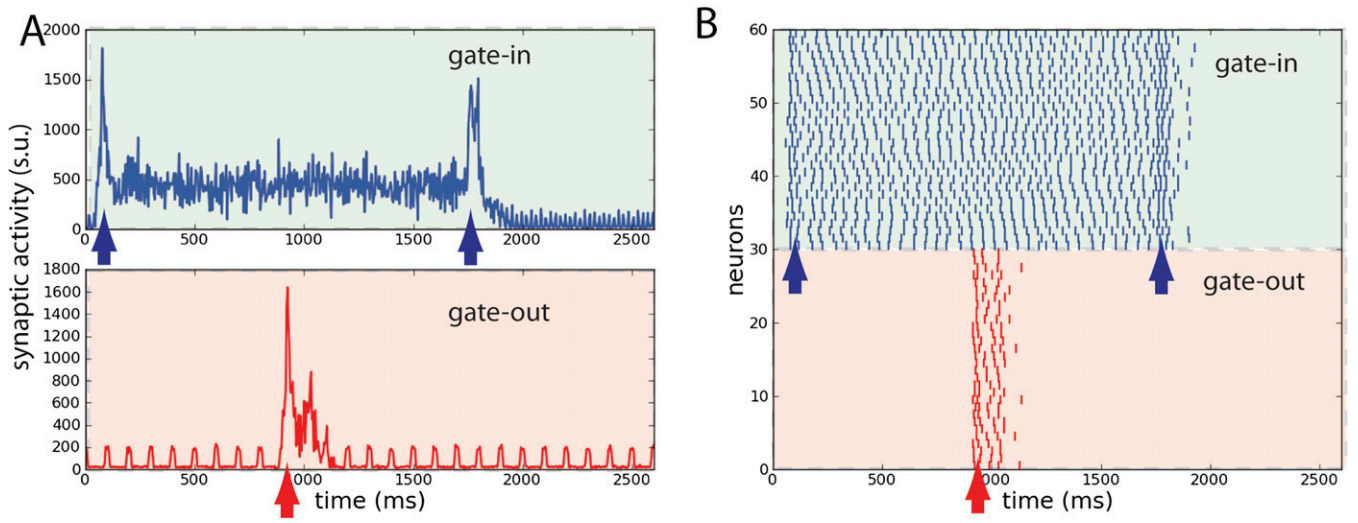

Fig. S6. Bihemispheric network with modulation of frequency only in space. (*A*) Average synaptic input of an example of a network performing correctly the DMS task of the population B (*Upper*) and population *R* (*Lower*). Colored area represents different values of oscillations frequency: $\nu_s = 45$ Hz (green) and $\nu_s = 10$ Hz (red). (*B*) Rastergram of 30 representative neurons for each population.

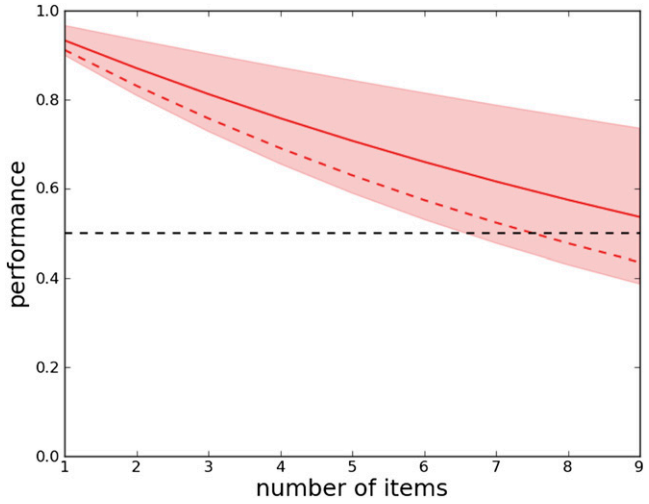

Fig. S7. Memory maintenance performance of our extended model as a function of the number of items to be retained. Continuous red line: performance for maintenance probability of the single population $P_m^1 = 0.93$ (red shadowed area: error). Dashed red line: performance with maintenance probability of the single population $P_m^1 = 0.91$.